RESEARCH ARTICLE | MARCH 18 2025

Photoplastic anisotropy in nanoindentation of wurtzite ZnO single crystals

Hiroto Oguri ; Yan Li ; Xufei Fang ; Atsutomo Nakamura

Appl. Phys. Lett. 126, 114101 (2025)
https://doi.org/10.1063/5.0248543

Applied Physics Letters ARTICLE pubs.aip.org/aip/apl

Photoplastic anisotropy in nanoindentation of wurtzite ZnO single crystals

Cite as: Appl. Phys. Lett. **126**, 114101 (2025); doi: 10.1063/5.0248543
Submitted: 12 November 2024 · Accepted: 7 February 2025 ·
Published Online: 18 March 2025

View Online Export Citation CrossMark

Hiroto Oguri,[1,2] Yan Li,[1] Xufei Fang,[1,2,a)] and Atsutomo Nakamura[1,a)]

AFFILIATIONS

[1]Department of Mechanical Science and Bioengineering, Osaka University, Toyonaka, Osaka 560-8531, Japan
[2]Institute for Applied Materials, Karlsruhe Institute of Technology, Kaiserstrasse 12, 76131 Karlsruhe, Germany

[a)]**Authors to whom correspondence should be addressed:** xufei.fang@kit.edu and a.nakamura.es@osaka-u.ac.jp

ABSTRACT

Anisotropy plays a crucial role in understanding and optimizing the properties of materials with directional dependencies. The hexagonal wurtzite structure, which is a typical crystal structure in compound semiconductors, demonstrates pronounced anisotropy, especially in its response to external stimuli. Recently, mechanical behavior under light illumination has attracted increasing interest especially in semiconductor compounds. In this study, we investigated the anisotropy of illumination effects on the nanomechanical properties of wurtzite ZnO. Four surface orientations—(0001), (0001) 45° off, $(1\bar{1}00)$, and $(2\bar{1}\bar{1}0)$—were subjected to nanoindentation creep and nanoindentation hardness tests under controlled light illumination. The indentation depth during nanoindentation creep under light illumination was consistently smaller than that in darkness for all surface orientations, confirming that light suppresses indentation creep deformation, but to different degrees depending on the surface orientation. This suggests that the activated slip systems and the distribution of dislocations play a crucial role in modulating dislocation behavior under light illumination. The nanoindentation hardness followed the trend on the four surface orientations: (0001) > (0001) 45° off > $(1\bar{1}00)$ > $(2\bar{1}\bar{1}0)$, reflecting anisotropic behavior in nanomechanical properties. Second and subsequent pop-in events were extracted, exhibiting different behaviors depending on the surface orientations, and may play a key role in determining the anisotropy in nanoindentation hardness. Our findings contribute to a comprehensive understanding of the plastic anisotropy under light control in wurtzite ZnO.

Compound semiconductors with wideband gaps, such as ZnO, GaN, ZnS, and SiC, have been recognized as promising candidates for future power electronics.[1] Most of these binary compound semiconductors crystallize in either cubic zinc-blend or hexagonal wurtzite structure. These structures are characterized by typical covalent bonding but also exhibit a substantial ionic character.[2] Consequently, compound semiconductors have long been considered brittle with limited plasticity, making them prone to brittle fracture at room temperature. Recently, experimental studies on cubic zinc-blend ZnS crystals have proven that the material can deform up to ~45% true strain in darkness even at room temperature during bulk compression,[3] and light illumination has a significant influence on the mobility of dislocations.[3,4] Photoindentation studies on ZnS highlight that controlling the light illumination can be a promising approach to enhance the dislocation-based plasticity of materials.[5] These growing interest in the influence of light illumination on the mechanical properties of compound semiconductors, referred to as the photoplastic effect,[6] to uncover the potential for improving their deformability and processing capabilities are worth pursuing further.

The wurtzite crystal structure, characteristic of materials such as ZnO and GaN, exhibits pronounced anisotropy due to its hexagonal system and lack of mirror symmetry along the [0001] axis. This anisotropy is reflected in the mechanical,[7–9] magnetic,[10] optical,[11] and electronic properties,[2,11] which vary significantly depending on the crystallographic orientations. For example, mechanical deformation in the [0001] direction differs substantially from that along the $[1\bar{1}00]$ or $[2\bar{1}\bar{1}0]$ directions,[12–14] with the [0001] axis typically showing higher hardness and different slip systems compared to other orientations.[12,15,16] Furthermore, piezoelectric effects, caused by the non-centrosymmetric nature of the structure, are also strongly anisotropic and more pronounced along the [0001] axis.[17,18] These anisotropic properties have critical implications for the design and optimization of devices, particularly in optoelectronics and piezoelectric applications.[18] Thus, a thorough understanding of the anisotropic characteristics of

wurtzite materials is essential for optimizing their performance in various technological applications.[19,20]

In this study, we investigated the anisotropy of illumination effects on the nanomechanical properties of wurtzite ZnO using the photoindentation technique.[5] Previous nanoindentation studies on wurtzite ZnO have primarily focused on the (0001) plane and used higher loads exceeding 10 mN.[21–26] Although there have been studies on the anisotropy of mechanical properties, most of them employed loads over 1 mN, and the comparison between the $(1\bar{1}00)$ plane and $(2\bar{1}\bar{1}0)$ plane did not yield consistent results.[12,13,27] Moreover, few studies have thoroughly examined the effects of illumination on the anisotropy of mechanical properties. In semiconductor materials, different types of dislocations (e.g., pyramidal dislocations, basal dislocations, prismatic dislocations) exhibit different core structures, leading to varied electrical behavior and potentially different responses to light illumination. In this study, we extracted the anisotropy of the photoplastic effect at the nanometer scale through photoindentation tests on ZnO (0001) plane, (0001) 45° off plane, $(1\bar{1}00)$ plane, and $(2\bar{1}\bar{1}0)$ plane under much lower loads (hundreds of μN). The results are critical for uncovering the photoplastic effect in wurtzite semiconductors.

The wurtzite ZnO single crystals used in this work were provided by ZENIYA INDUSTRY Inc., Japan. Four surface orientations were investigated: (0001) *c*-plane, (0001) 45° off *c*45°off-plane, $(1\bar{1}00)$ *m*-plane, and $(2\bar{1}\bar{1}0)$ *a*-plane, as schematically illustrated in Fig. 1. The term (0001) 45° off refers to the angle between loading axis ***P*** and [0001] being 45° [Fig. 1(b)]. All samples have a thickness of 1 mm to avoid sample compliance issue[28,29] during nanomechanical testing. Nanoindentation tests with controlled light illumination or *photoindentation*[5] tests were carried out at a constant temperature of 30 °C using an instrumented nanoindentation platform ENT-NEXUS (ELIONIX Inc., Japan), with a diamond Berkovich tip that has an effective tip radius of ~90 nm. All tests were carried out with the load-control mode. For more details about the photoindentation setup, refer to our previous studies.[5,16]

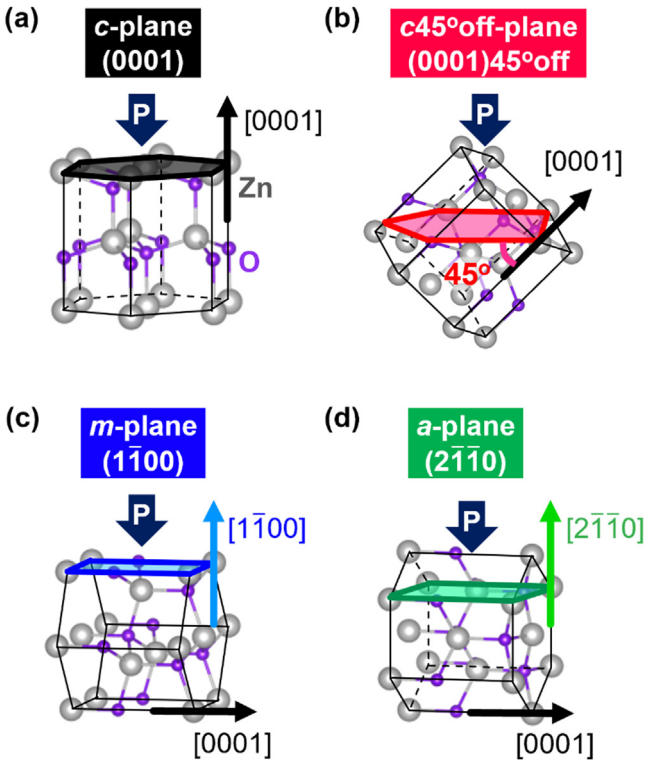

FIG. 1. Schematic illustrations of the sample orientations of (a) *c*-plane, (b) *c*45°off-plane, (c) *m*-plane, and (d) *a*-plane. Arrows with the letter ***P*** denote the loading axis, and the highlighted colored planes are indented.

Two types of nanoindentation tests were conducted on all the ZnO single crystals, namely, nanoindentation creep tests and nanoindentation hardness tests. In nanoindentation creep tests, a maximum load of 300 μN was maintained for 100 s, and upon unloading, a load of 30 μN (10% of the maximum load) was maintained for 100 s to assess the thermal drift, both in darkness and under light illumination. The drift was found to be less than 6.0×10^{-3} nm/s and has been calibrated into all nanoindentation creep curves. Ultraviolet (UV) light with a wavelength of 405 nm (which is just below the bandgap of ZnO, 3.3 eV at room temperature[2]) was employed for the maximum effect between light and darkness. A light intensity of 100 μW/cm^2 at the indenter tip was adopted as it is sufficient to interact with indentation-induced dislocations, according to the previous study.[16] In nanoindentation hardness tests, a maximum load of 200 μN was applied to the samples in complete darkness. The nanoindentation method allows for excellent statistical studies with repetitive tests under the same conditions, and the number of valid indentations per set of tests for the two experiment types is 30 and 80, respectively.

Figure 2 demonstrates the average indentation depth as a function of holding time both in darkness and in light for four surface orientations during nanoindentation creep tests. Each curve was obtained by averaging at least 30 curves to ensure reliable data for statistical analysis. The shaded regions with the same color as the solid lines correspond to the standard deviation bands. The standard deviations, calculated from at least 30 data points, were less than 1.1 nm, indicating excellent reproducibility of the experiments regardless of surface orientations and light conditions. The differences between indentation depth in darkness and in light for four surface orientations are revealed to be statistically significant by Welch's *t*-test.[30] More details on the statistical test are provided in the supplementary material Sec. 4. The stress exponents in darkness and in light calculated from the experiments indicate that the dominant mechanism of indentation creep is dislocation creep regardless of surface orientations, as detailed in the supplementary material Sec. 2. It should be noted that the indentation depth in 405 nm light is always smaller than that in darkness, implying the effects of light illumination on dislocation motion regardless of surface orientations. Such photoplastic effect in nanoindentation creep on $(1\bar{1}00)$ *m*-plane [Fig. 1(c)] and $(2\bar{1}\bar{1}0)$ *a*-plane [Fig. 1(d)] have not been reported before. The effect of light observed in nanoindentation on (0001) *c*-plane [Fig. 1(a)] and (0001) 45° off *c*45°off-plane [Fig. 1(b)] is consistent with our previous nanoindentation results.[15,16,31] The difference in indentation depth in each light condition between this study and previous studies on *c*-plane[15] and *c*45°off-plane[16] might be derived from the difference in the tip radius of the indenter.

We also observed that the effect of light on nanoindentation creep behavior varied depending on the surface orientation. The average indentation depth at $t = 100$ s under light illumination is 3.2%, 9.0%,

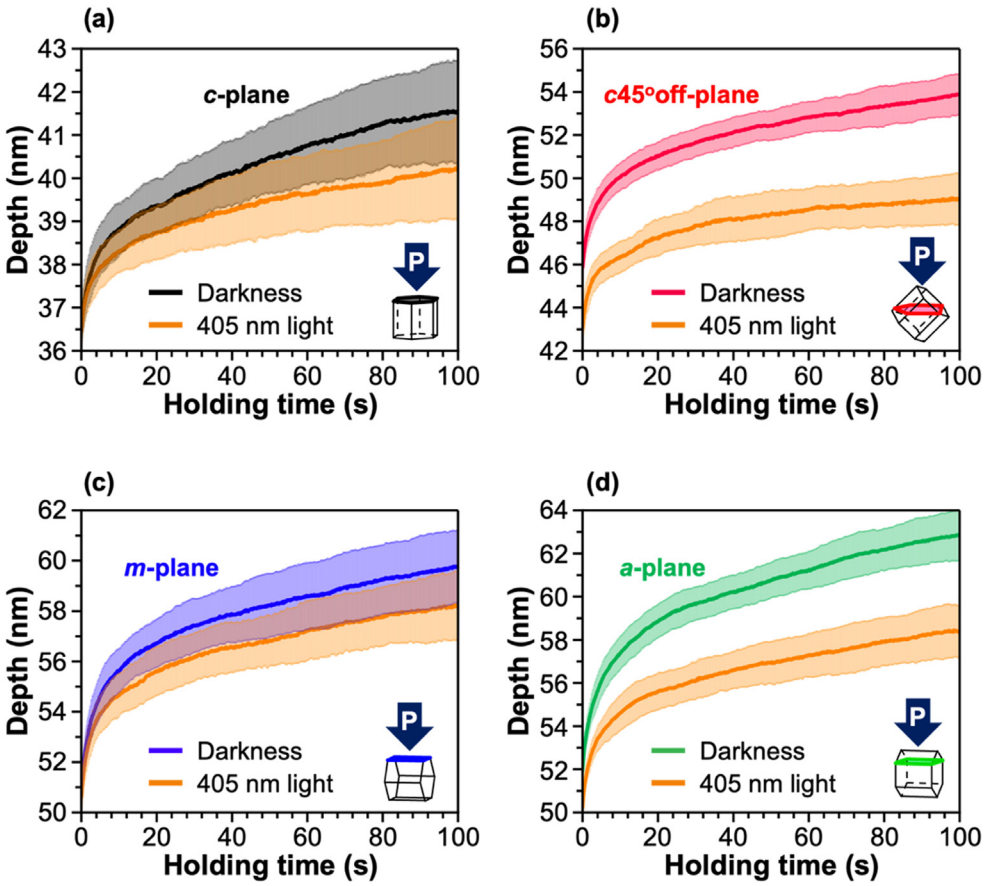

FIG. 2. Nanoindentation depth as a function of holding time in darkness and in 405 nm light obtained by 300 μN nanoindentation creep tests on (a) *c*-plane, (b) *c*45°off-plane, (c) *m*-plane, and (d) *a*-plane.

2.6%, and 7.2% smaller than that in darkness for *c*-plane, *c*45°off-plane, *m*-plane, and *a*-plane, respectively. The photoplastic effect is proposed to arise from the interaction between photo-excited carriers (electrons and holes) and dislocations. Matsunaga *et al.* have reported that dislocations in compound semiconductors can trap these carriers through localized electrostatic fields around their cores, leading to the reconstruction of chemical bonds near the cores.[32,33] This results in an increased Peierls potential barrier and a reduced indentation creep rate associated with dislocation mobility. Therefore, the difference of indentation depth between in the dark and in light increases with the holding time. For nanoindentation on *c*-plane and *c*45°off-plane of ZnO, we reported that pyramidal[15] and basal slip systems[16] were activated, respectively. In indentation on the *m*-plane of ZnO, prismatic slip was predominantly observed, with some evidence of both basal and pyramidal slip as shown in Fig. S2. Coleman *et al.* demonstrated that both basal and pyramidal slip systems were activated after 50 mN nanoindentation on *a*-plane of ZnO. Therefore, it is noteworthy that nanoindentation on different surface orientations may lead to distinct dislocation distributions beneath the indents due to the activation of different slip systems, and the degree of suppression by illumination on dislocation motion can vary accordingly. The possible slip systems activated after indentation on the four surface orientations are illustrated in Fig. S3 in the supplementary material Sec. 2.

Figure 3 depicts the average indentation creep depth as a function of holding time in darkness for four surface orientations. Indentation creep depth refers to the change in indentation depth during the holding load. The small standard deviations make the minor differences in indentation creep depth across the four surface orientations statistically significant and comparable. The significance of the differences in creep depth at 100 s for different surface orientations are validated by Welch's *t*-test.[30] More details can be found in Sec. 4 of the supplementary material. As demonstrated in Fig. 3, indentation creep depth was largest for the *a*-plane, followed by the *m*-plane, *c*45°off-plane, and *c*-plane. This indicates that *a*-plane is the softest, and *c*-plane is the hardest in four surface orientations. Since the creep depth exhibits significant differences due to anisotropy, nanoindentation hardness tests were further conducted to identify the trend using nominal nanoindentation hardness (NI hardness) data. Additionally, minor differences in the trends between creep depth and nanoindentation hardness were discussed. Figure 4 presents typical load (*P*)-displacement (*h*) curves obtained from nanoindentation hardness tests on four surface orientations in darkness. 80 *P*-*h* curves for each surface orientation can be

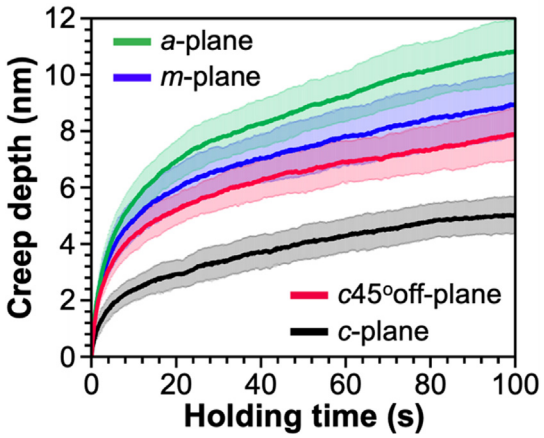

FIG. 3. Nanoindentation creep depth as a function of holding time obtained in darkness on *c*-plane, *c*45°off-plane, *m*-plane, and *a*-plane.

found in Fig. S4 in Sec. 3 of the supplementary material. Table I summarizes the mechanical properties calculated using the Oliver–Pharr method[29] and averaged from 80 data points for each surface orientation. As can be seen from the standard deviation of less than 1.2 nm in maximum depth, nanoindentation hardness tests are highly reproducible for all surface orientations. The NI hardness was highest for the *c*-plane, followed by the *c*45°off-plane, *m*-plane, and *a*-plane, which is noteworthy as it aligns excellently with the order of creep depth (Fig. 3). These trends directly result from the types of slip systems activated, which significantly influence hardness anisotropy. However, it should be noted that there are minor differences in the trends between creep depth and nominal NI hardness. The creep depth of the *m*-plane is closer to that of the *c*45°off-plane than the *a*-plane, whereas the nominal NI hardness of the *m*-plane is closer to that of the *a*-plane than the *c*45°off-plane. Creep depth reflects the indentation creep behavior during the holding load and may be related to dislocation mobility. In contrast, NI hardness under the same load is directly

TABLE I. The maximum depth and NI hardness averaged from 80 valid indentation tests for each surface orientation.

Orientation	*c*-plane	*c*45°off-plane	*m*-plane	*a*-plane
Maximum depth (nm)	27.5 ± 0.6	35.9 ± 1.1	39.3 ± 1.0	40.4 ± 1.1
NI hardness (GPa)	6.32 ± 0.31	3.67 ± 0.21	3.12 ± 0.14	2.92 ± 0.14

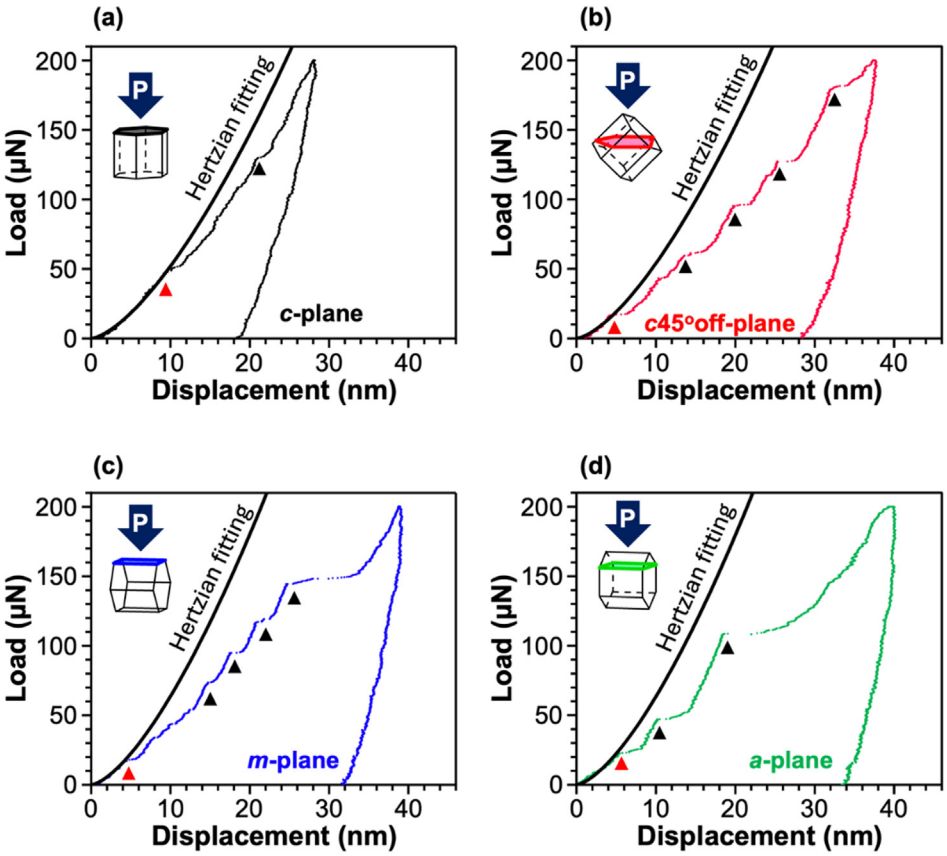

FIG. 4. Representative load-displacement (*P*-*h*) curves in darkness obtained by 200 μN nanoindentation hardness tests on (a) *c*-plane, (b) *c*45°off-plane, (c) *m*-plane, and (d) *a*-plane. The loading rate was 20 μN/s.

related to the indentation depth, which reflects the indentation deformation behavior during loading. The nominal NI hardness values obtained in this study are higher than the value of 5.0 GPa for *c*-plane at the indentation depth of 300 nm reported by Kucheyev *et al.*,[22] and 4.8 GPa for *c*-plane and 2.0 GPa for *a*-plane at the indentation depth of 50 nm reported by Coleman *et al.*,[34] which can be attributed to the smaller tip radius of the indenter and the much shallower indentation depth used here, consistent with the indentation size effect.[17,18]

To further analyze minor differences in the trends between creep depth and nominal NI hardness, indentation deformation behavior during loading in *P-h* curves from nanoindentation hardness tests was investigated. For all surface orientations, the elastic segment of the *P-h* curves prior to the first pop-in can be described by the Hertzian elastic contact theory,[35] indicated by the black solid curve in Fig. 4. The Hertzian fitting curves vary by surface orientation due to differences in the Young's modulus, which is 141.5 ± 4.0 GPa for the *c*-plane, 148.6 ± 6.2 GPa for the *c*45°off-plane, and 169.6 ± 11.3 GPa for the *m*-plane, 168.8 ± 7.9 GPa for the *a*-plane based on the nanoindentation tests. Pop-in events (denoted by the red and black triangles in Fig. 4) were clearly detected as a displacement burst at a constant load. The first pop-in events are often related to pressure-induced phase transformation,[36] crack formation,[37] or the transition from the elastic to the elastoplastic deformation.[38] Here, in ZnO single crystals, the first pop-in events, denoted by red triangles in Fig. 4, correspond to the onset of plasticity since previous indentation studies on this material have shown neither phase transformation nor cracking, even under a load of 100 mN.[39] The calculated maximum shear stress corresponding to the first pop-in events by Hertzian elastic contact theory[35] almost reaches the theoretical shear strength of $G/2\pi$; hence, these first pop-in events suggest homogeneous dislocation nucleation mechanism.[38,40] The cumulative probabilities as a function of the maximum shear stress at first pop-in events indicate the anisotropy of dislocation nucleation in ZnO, as shown in Fig. S5. More details on the calculations are provided in the supplementary material Sec. 3.

It should be noted that the second and subsequent pop-in behaviors, denoted by black triangles in Fig. 4, vary depending on the surface orientation. In the previous nanoindentation studies on ZnO, clear second and subsequent pop-in behaviors have not been fully understood. In this study, using a nanoindenter with an effective tip radius of 90 nm and a small loading rate of 20 μN/s, we extracted distinct second and subsequent pop-in behaviors. For *c*- and *c*45°off-planes, the clear second and subsequent pop-in events during the loading to 200 μN were mostly displacement bursts that were equal to or smaller than the first pop-in event. In contrast, *m*- and *a*-planes exhibited much larger displacement burst than the first pop-in at some points during the second and subsequent pop-in events when loading up to 200 μN. This variation in the second and subsequent pop-in behaviors may be attributed to the minor differences in the trends between creep depth and NI hardness observed in this study. Creep depth reflects the indentation creep behavior during the holding load and may be related to dislocation mobility in activated slip systems. In contrast, NI hardness under the same load is directly related to the indentation depth, which reflects the deformation behavior during loading. Therefore, NI hardness may be influenced not only by dislocation mobility but also by the elastic modulus and subsequent pop-in behavior. As mentioned above, the trend in the Young's modulus obtained from the Oliver–Pharr method indicates that *c*-plane shows the smallest value, while both *a*- and *m*-planes show the largest. This suggests that the influence of the Young's modulus on the trend differences in NI hardness and creep depth among the *c*45°off-plane, *m*-plane, and *a*-plane may not be substantial. Hence, the NI hardness can be significantly influenced not only by the mobility of dislocations in activated slip systems and the elastic modulus of materials but also by the length of displacement bursts caused by multiple pop-in events during loading. Second and subsequent pop-in events can be related to the evolution of the dislocation network.[41] As stated earlier, indentation on ZnO revealed the activation of pyramidal slip on the *c*-plane,[15] basal slip on the *c*45°off-plane,[16] prismatic slip with some evidence of both basal and pyramidal slip on the *m*-plane, and both basal and pyramidal slip on the *a*-plane. Therefore, the much larger displacement bursts than the first pop-in observed on the *m*-plane and *a*-plane [Figs. 4(c) and 4(d)] may correspond to significant evolution of the dislocation network driven by the interaction of multiple slip systems. However, this topic would require extensive *in situ* TEM studies and advanced simulations, and therefore, it will be investigated in the future work.

To summarize, in this study, we performed photoindentation tests to investigate the effects of light illumination as well as the anisotropy on nanoindentation behavior of wurtzite ZnO single crystals for four surface orientations: *c*-plane, *c*45°off-plane, *m*-plane, and *a*-plane. The photoplastic effect of nanoindentation on *m*-plane and *a*-plane was observed. The indentation depth during nanoindentation creep under light illumination was consistently smaller than that in darkness for all surface orientations, confirming that light illumination suppresses dislocation mobility as reflected in the indentation creep deformation, with different degrees depending on the surface orientation. The variation in photoplastic effects across surface orientations suggests that the activated slip systems and the distribution of dislocations play a crucial role in modulating dislocation behavior under light illumination. The indentation creep depth obtained in darkness was largest for the *a*-plane, indicating its relative softness, while the *c*-plane exhibited the smallest indentation creep depth, correlating with its higher hardness, as confirmed by the nanoindentation hardness tests. Second and subsequent pop-in events were extracted using an indenter with a small tip radius and low loading rate. The *c*-plane and *c*45°off-plane predominantly exhibited displacement bursts equal to or smaller than the first pop-in event, whereas the *m*-plane and *a*-plane demonstrated much larger displacement bursts, possibly due to the activation of multiple slip systems. This suggests that nanoindentation hardness can be influenced not only by the mobility of activated dislocations but also by the magnitude of displacement bursts caused by multiple pop-in events during loading. This research provides further understanding of the photoplastic effects and nanoindentation hardness in wurtzite ZnO.

See the supplementary material for details on the dominant mechanism of nanoindentation creep, possible slip planes activated after indentation on four surface orientations of ZnO, cumulative distribution of maximum shear stresses at first pop-in events, statistical test to check the significance of the differences, and anisotropy of nanoindentation creep behavior in 405 nm light.

This work was financially supported by the JSPS KAKENHI (Grant Nos. JP24H00285, JP24K17169, and JP24H00032), Japan. X.

F. acknowledges the support by the European Union (ERC, Project MECERDIS, Grant No. 101076167). Views and opinions expressed are, however, those of the authors only and do not necessarily reflect those of the European Union or the European Research Council. Neither the European Union nor the granting authority can be held responsible for them. H. Oguri acknowledges the financial support by the JST, the establishment of university fellowships toward the creation of science technology innovation (Grant No. JPMJFS2125).

AUTHOR DECLARATIONS

Conflict of Interest

The authors have no conflicts to disclose.

Author Contributions

Hiroto Oguri: Conceptualization (equal); Formal analysis (equal); Investigation (equal); Writing – original draft (equal). **Yan Li:** Conceptualization (equal); Funding acquisition (lead); Writing – review & editing (equal). **Xufei Fang:** Conceptualization (equal); Funding acquisition (lead); Writing – review & editing (equal). **Atsutomo Nakamura:** Conceptualization (equal); Funding acquisition (lead); Project administration (lead); Supervision (lead); Writing – review & editing (equal).

DATA AVAILABILITY

The data that support the findings of this study are available from the corresponding authors upon reasonable request.

REFERENCES

[1]F. Roccaforte, P. Fiorenza, G. Greco, R. Lo Nigro, F. Giannazzo, F. Iucolano, and M. Saggio, "Emerging trends in wide band gap semiconductors (SiC and GaN) technology for power devices," Microelectron. Eng. **187-188**, 66–77 (2018).
[2]Ü. Özgür, Y. I. Alivov, C. Liu, A. Teke, M. A. Reshchikov, S. Doğan, V. Avrutin, S. J. Cho, and H. Morkoç, "A comprehensive review of ZnO materials and devices," J. Appl. Phys. **98**, 041301 (2005).
[3]Y. Oshima, A. Nakamura, and K. Matsunaga, "Extraordinary plasticity of an inorganic semiconductor in darkness," Science **360**(6390), 772–774 (2018).
[4]Y. Oshima, A. Nakamura, K. P. D. Lagerlöf, T. Yokoi, and K. Matsunaga, "Room-temperature creep deformation of cubic ZnS crystals under controlled light conditions," Acta Mater. **195**, 690–697 (2020).
[5]A. Nakamura, X. Fang, A. Matsubara, E. Tochigi, Y. Oshima, T. Saito, T. Yokoi, Y. Ikuhara, and K. Matsunaga, "Photoindentation: A new route to understanding dislocation behavior in light," Nano Lett. **21**(5), 1962–1967 (2021).
[6]Y. Osip'yan and I. B. Savchenko, "Experimental observation of the influence on plastic deformation of cadmium sulfide," JETP Lett. **7**(4), 130–134 (1968).
[7]W. Wang and K. Lu, "Nanoindentation study on elastic and plastic anisotropies of Cu single crystals," Philos. Mag. **86**, 5309–5320 (2006).
[8]S. Bhagavat and I. Kao, "Nanoindentation of lithium niobate: Hardness anisotropy and pop-in phenomenon," Mater. Sci. Eng., A **393**(1–2), 327–331 (2005).
[9]W. Wang and K. Lu, "Nanoindentation measurement of hardness and modulus anisotropy in Ni_3Al single crystals," J. Mater. Res. **17**(9), 2314–2320 (2002).
[10]U. Welp, V. K. Vlasko-Vlasov, X. Liu, J. K. Furdyna, and T. Wojtowicz, "Magnetic domain structure and magnetic anisotropy in $Ga_{1-x}Mn_xAs$," Phys. Rev. Lett. **90**(16), 167206 (2003).
[11]N. Ueda, H. Hosono, R. Waseda, and H. Kawazoe, "Anisotropy of electrical and optical properties in β-Ga_2O_3 single crystals," Appl. Phys. Lett. **71**(7), 933–935 (1997).
[12]T. H. Sung, J. C. Huang, and H. C. Chen, "Mechanical response of polar/non-polar ZnO under low dimensional stress," Appl. Phys. Lett. **102**(24), 241901 (2013).
[13]P. H. Lin, X. H. Du, Y. H. Chen, H. C. Chen, and J. C. Huang, "Nano-scaled diffusional or dislocation creep analysis of single-crystal ZnO," AIP Adv. **6**(9), 095125 (2016).
[14]T. H. Sung, J. C. Huang, J. H. Hsu, S. R. Jian, and T. G. Nieh, "Yielding and plastic slip in ZnO," Appl. Phys. Lett. **100**, 211903 (2012).
[15]H. Oguri, Y. Li, E. Tochigi, X. Fang, K. Tanigaki, Y. Ogura, K. Matsunaga, and A. Nakamura, "Bringing the photoplastic effect in ZnO to light: A photoindentation study on pyramidal slip," J. Eur. Ceram. Soc. **44**(2), 1301–1305 (2024).
[16]Y. Li, X. Fang, E. Tochigi, Y. Oshima, S. Hoshino, T. Tanaka, H. Oguri, S. Ogata, Y. Ikuhara, K. Matsunaga, and A. Nakamura, "Shedding new light on the dislocation-mediated plasticity in wurtzite ZnO single crystals by photoindentation," J. Mater. Sci. Technol. **156**, 206–216 (2023).
[17]S. Abubakar, S. T. Tan, J. Y. C. Liew, Z. A. Talib, R. Sivasubramanian, C. A. Vaithilingam, S. S. Indira, W. C. Oh, R. Siburian, S. Sagadevan, and S. Paiman, "Controlled growth of semiconducting ZnO nanorods for piezoelectric energy harvesting-based nanogenerators," Nanomaterials **13**(6), 1025 (2023).
[18]V. Consonni and A. M. Lord, "Polarity in ZnO nanowires: A critical issue for piezotronic and piezoelectric devices," Nano Energy **83**, 105789 (2021).
[19]J. Zúñiga-Pérez, V. Consonni, L. Lymperakis, X. Kong, A. Trampert, S. Fernández-Garrido, O. Brandt, H. Renevier, S. Keller, K. Hestroffer, M. R. Wagner, J. S. Reparaz, F. Akyol, S. Rajan, S. Rennesson, T. Palacios, and G. Feuillet, "Polarity in GaN and ZnO: Theory, measurement, growth, and devices," Appl. Phys. Rev. **3**(4), 041303 (2016).
[20]S. Takahashi, A. Kan, H. Ogawa, and C. Noguera, "Polar oxide surfaces," J. Phys.: Condens. Matter **12**, R367–410 (2000).
[21]J. E. Bradby, S. O. Kucheyev, J. S. Williams, C. Jagadish, M. V. Swain, P. Munroe, and M. R. Phillips, "Contact-induced defect propagation in ZnO," Appl. Phys. Lett. **80**(24), 4537–4539 (2002).
[22]S. O. Kucheyev, J. E. Bradby, J. S. Williams, C. Jagadish, and M. V. Swain, "Mechanical deformation of single-crystal ZnO," Appl. Phys. Lett. **80**(6), 956–958 (2002).
[23]V. A. Coleman, J. E. Bradby, C. Jagadish, and M. R. Phillips, "A comparison of the mechanical properties and the impact of contact induced damage in a- and c- axis ZnO single crystals," in *2006 MRS Fall Meeting* (MRS, 2007), pp. 213–218.
[24]S. Basu and M. W. Barsoum, "Deformation micromechanisms of ZnO single crystals as determined from spherical nanoindentation stress-strain curves," J. Mater. Res. **22**(9), 2470–2477 (2007).
[25]S. R. Jian, "Mechanical responses of single-crystal ZnO," J. Alloys Compd. **494**(1–2), 214–218 (2010).
[26]Y. J. Kim, I. C. Choi, J. A. Lee, M. Y. Seok, and J. I. Jang, "Strain-dependent transition of time-dependent deformation mechanism in single-crystal ZnO evaluated by spherical nanoindentation," Philos. Mag. **95**(16–18), 1896–1906 (2015).
[27]R. Juday, E. M. Silva, J. Y. Huang, P. G. Caldas, R. Prioli, and F. A. Ponce, "Strain-related optical properties of ZnO crystals due to nanoindentation on various surface orientations," J. Appl. Phys. **113**(18), 183511 (2013).
[28]M. F. Doerner and W. D. Nix, "A method for interpreting the data from depth-sensing indentation instruments," J. Mater. Res. **1**(4), 601–609 (1986).
[29]W. C. Oliver and G. M. Pharr, "An improved technique for determining hardness and elastic modulus using load and displacement sensing indentation experiments," J. Mater. Res. **7**(6), 1564–1583 (1992).
[30]B. L. Welch, "The generalization of student's problem when several different population variances are involved," Biometrika **34**(1–2), 28–35 (1947).
[31]H. Oguri, Y. Li, and A. Nakamura, "A nanoindentation approach for unveiling the photoplastic effects by a 'light switch': A case study on ZnO," J. Am. Ceram. Soc. e20338 (2024).
[32]K. Matsunaga, S. Hoshino, M. Ukita, Y. Oshima, T. Yokoi, and A. Nakamura, "Carrier-trapping induced reconstruction of partial-dislocation cores responsible for light-illumination controlled plasticity in an inorganic semiconductor," Acta Mater. **195**, 645–653 (2020).
[33]S. Hoshino, Y. Oshima, T. Yokoi, A. Nakamura, and K. Matsunaga, "DFT calculations of carrier-trapping effects on atomic structures of 30° partial

dislocation cores in zincblende II-VI group zinc compounds," Phys. Rev. Mater. **7**(1), 013603 (2023).
[34]V. A. Coleman, J. E. Bradby, C. Jagadish, P. Munroe, Y. W. Heo, S. J. Pearton, D. P. Norton, M. Inoue, and M. Yano, "Mechanical properties of ZnO epitaxial layers grown on a- and c-axis sapphire," Appl. Phys. Lett. **86**(20), 203105 (2005).
[35]K. L. Johnson, *Contact Mechanics* (Cambridge University Press, 1987).
[36]R. Abram, D. Chrobak, and R. Nowak, "Origin of a nanoindentation pop-in event in silicon crystal," Phys. Rev. Lett. **118**, 95502 (2017).
[37]X. Fang, H. Bishara, K. Ding, H. Tsybenko, L. Porz, M. Höfling, E. Bruder, Y. Li, G. Dehm, and K. Durst, "Nanoindentation pop-in in oxides at room temperature: Dislocation activation or crack formation?," J. Am. Ceram. Soc. **104**(9), 4728–4741 (2021).
[38]J. R. Morris, H. Bei, G. M. Pharr, and E. P. George, "Size effects and stochastic behavior of nanoindentation pop in," Phys. Rev. Lett. **106**(16), 165502 (2011).
[39]S. R. Jian, "Pop-in effects and dislocation nucleation of c-plane single-crystal ZnO by Berkovich nanoindentation," J. Alloys Compd. **644**, 54–58 (2015).
[40]X. Fang, L. Porz, K. Ding, and A. Nakamura, "Bridging the gap between bulk compression and indentation test on room-temperature plasticity in oxides: Case study on $SrTiO_3$," Crystals **10**(10), 933 (2020).
[41]Y. Sato, S. Shinzato, T. Ohmura, T. Hatano, and S. Ogata, "Unique universal scaling in nanoindentation pop-ins," Nat. Commun. **11**(1), 4177 (2020).